FINAL REPORT ON

OSCILLATORY INTERACTION OF SOLID PROPELLANT COMBUSTION AND COMBUSTOR FLOW

Thiokol Purchase Order No. 0790

June 1990

E. W. Price, K. Prasad, C. Markou
School of Aerospace Engineering
Georgia Institute of Technology
Atlanta, Georgia 30332

INTRODUCTION

Effort this year has been devoted to the following topics:

1. Rigorous modeling of a two-dimensional diffusion flame, development of a computer code, and use of the code to study the leading edge portion of the flame that dominates upstream heat transfer.

2. Experimental determination of the width of the "smooth band" on the AP surface of edge burning sandwiches (as a function of binder lamina thickness and pressure). This is a needed input to the Deur-Price response function model.

3. Completion of the survey of L^* Instability.

4. Beginning of a study of the combustion of edge burning sandwiches in which the binder lamina is partially filled with particulate AP (to study the interaction between O/F flames on coarse and fine particles).

A short summary of each study follows. The majority of the effort has been on #1, which is now producing important details of diffusion flame structure not previously obtainable.

DIFFUSION FLAME ANALYSIS

A critical part of the combustion zone of a heterogeneous solid propellant is that portion of the oxidizer-fuel diffusion flamelets that is closest to the burning surface. This leading edge of the flamelet dominates the heat feedback to the surface, and hence is important to overall combustion characteristics. Unfortunately, there has been no adequate analytical model of this part of the flame, and it is too small to study experimentally. The Georgia Tech team has been addressing this problem by an Office of Naval Research-sponsored experimental study using a gas burner operated at atmospheric pressure. Methane and air were chosen as reactants because of the large amount of kinetic data pertaining to the elementary reactions involved in methane-air combustion. Under the Thiokol Contract, development of a computer code for solution of the

corresponding two-dimensional diffusion flame problem was undertaken. The code is relatively general in that it accommodates:

a) any combination of reactants for which pertinent reaction kinetic data are available (for elementary reactions)
b) viscous effects
c) temperature dependence of transport properties
d) one, or two dimensions
e) nonsteady behavior

As presently operated, the program is for (rectangular) 2-D flames, with uniform inlet flow and side boundary conditions corresponding to symmetry with an identical burner flow on each side.

The computer code was first run in complete form on the Pittsburgh Supercomputing Center Cray YMP computer in January 1990, after a long period of checking out subroutines on smaller computers, and preliminary runs on 1-D flames. Since then extensive effort has been devoted to modifications to reduce time and cost of computer runs, and to analysis of results from the first run. In this effort, we have been supported by grants of computer time from NSF and ONR. The time requirements for steady state solutions are now small enough for limited parametric studies of flame behavior, which will be done first for the methane-air system. Computational time is strongly dependent on the number of reaction equations and species; we have not yet begun to look at systems more complex than methane and air, but it is clear that these rigorous solutions will be computer time-intensive. However, we are already gaining a great deal of physical insight from results to date, and it is clear that previous approximate analytical representations of such flames are wholly inadequate for the leading edge part of that flame.

Some of the results of the first complete solution are shown in Fig. 1 to 8. In these figures the oxidizer and fuel enter and start mixing at the coordinate baseline on the lower left; the x distance out to the upper right is height above the burner surface. Along the left-hand scale, pure air enters at low and high y, with the fuel flow entering in between. The third coordinate is the magnitude of the computed variable (species concentration, heat release rate,

pressure, velocity). From an examination of the figures shown, it is evident that the leading edge flame is the site of extraordinarily high heat release rate, so high that a local pressure rise occurs there, causing the approach flow to diverge. The heat flow upstream is localized, and dependent on two dimensional details of convection, conduction, and heat release distribution.

In the future, solutions will be run for different inflow velocities; of particular interest will be the relation between the upstream heat flow field and flow velocity, which determine burning rate in propellant combustion. Later solutions will replace the specification of inflow velocity by pyrolysis rates of solid oxidizer and fuel, determined by the calculated upstream heat flow (simulating propellant combustion). We are also anxious to get on with oscillatory solutions, but are limited by the computer time required.

SMOOTH BAND WIDTH

Studies of combustion of heterogeneous AP propellants have revealed (Ref. 1) a complex thermal interaction between oxidizer and binder in the thin subsurface region close to the AP-binder contact surfaces. In this region, the AP surface is hotter than the binder surface, and heat flows from the oxidizer into the binder. The small region of AP that experiences this heat "drain" into the binder decomposes differently than the rest of the AP surface. This difference is revealed as a "smooth band" on the AP surface around the outer periphery of the oxidizer surfaces on quenched samples (Fig. 9). This is an important feature of the combustion, because this portion of the AP surface decomposes endothermally by dissociative sublimation, whereas the rest of the surface decomposes exothermally in a surface froth layer (the smooth band region typically protrudes relative to the rate-determining region at the outer edge of the smooth band).

In the Deur-Price model for oscillatory combustion (Ref. 2), the outer edge of the smooth band has been taken as an indication of the outer limit of the flow that participates in the leading edge portion of the diffusion flamelet. Thus, the model requires experimental input regarding the width of the smooth band. A series of interrupted burning tests have now been completed on AP-PBAN binder sandwiches, permitting measurement of smooth band width. Fig. 10 shows two

quenched samples, and the collected results of 80 tests are shown in Fig. 11 and Table 1. The tests included a pressure range of 100 to 1200 psi and a range of binder lamina thickness of 20 to 200 μm. Test samples were made with AP laminae cleaved from single AP crystals, and also with AP laminae made by dry-pressing AP powder (results were about the same).

Some features of the quenched samples deserve mention before discussion of the trends of smooth band width. The outer boundary of the smooth band is irregular, and its location was measured by visual fitting of an average line through the irregularities. Also, many of the samples showed differences in the smooth bands on opposite AP laminae. The differences were consistently correlated with two other features of the sample (Fig. 10a). The unsymmetrical samples exhibited a separation of the oxidizer and binder on one side. The AP protruded less at that interface, and the smooth band was narrower. With one sample, the detachment switched from one side to the other, Fig. 12, and the corresponding smooth band features switched accordingly. No evidence of reaction in the separation gap could be seen. It was concluded that the gap resulted from mechanical separation at the moment of quench, and that some continued AP surface reaction occurred on the lamina on the separated side during quench because of removal of the binder heat sink by detachment. The data on smooth band width reported here is for the unseparated side of the sandwich.

Examination of Fig. 11 shows that smooth band width is a strong function of binder thickness and a weak function of test pressure. Results with single crystal AP laminae and pressed AP laminae were not significantly different.

The increasing smooth band width with increasing binder thickness is indicative of

a) The increased heat drain from AP lamina to binder lamina as the size of the binder heat sink increases

b) Shift of the stoichiometric surface, and hence of the leading edge flame further from the lamina contact plane, outward over the AP

lamina, because of larger fuel vapor flow (more fuel-rich diffusion field).

Lower smooth band width at higher pressure is probably due to a combination of factors, the most obvious being the thinner thermal wave in the solid at high pressure.

L^* INSTABILITY

The original objective of this study was to determine the extent to which experimental observations of L^* instability could be explained by a combination of a combustor model based simply on mass-balance and the relatively simple "QSHOD" model of dynamic combustion response (e.g., the Dennison and Baum model) (Ref. 3). This objective was stimulated by an observation that failure of the elementary theory to explain various experimental results had been the basis for pursuit of more exotic response function and combustor models in the last 20 years. Review of reports of failure of the theory had shown that the applicability of the elementary theory had not been fully evaluated before being declared "inadequate", raising a question about the necessity for that research that had followed to resolve the inadequacy. While the elementary theory has recognized shortcomings, its adequacy should be fully tested before its "failure" is used as a justification for excursions into more complex theory.

In reviewing the elementary theory, it was found that certain correlations of experimental variables were particularly useful as tests of the theory. In most published works, these correlations were not the ones chosen for presentation of results, so the theory was not put to test and meaningful conclusions could not be drawn. Even more important, it was found that data ordinarily taken was not sufficient to test even the elementary theory. In particular , it is necessary to make a determination of the growth rate of oscillations to test the theory fully, and most investigators did not do that. To illustrate the importance of that information, Fig. 13 shows a plot of $L^* (\bar{r})^2$ vs Ω for test results by Boggs, et al in Ref. 4 (which included measurements of α). The elementary theory predicts (Ref. 3) that $L^* (\bar{r})^2$ and Ω have unique values at the stability limit where $\alpha = 0$. Within the limits of the small perturbation elementary model, results for different values of α should fall on a

single curve $L^* (\bar{r})^2$, usually with lower $L^* (\bar{r})^2$ and higher Ω at higher α. The results in Fig. 13 conform fairly well to this trend, although there is a weak dependence on pressure indicated. In this correlation of data, the elementary theory provides a rational explanation for a trend of data away from the stability limit, which is somewhere at the upper left. Most investigators don't even measure α, and thus have a major trend in their data that is explained by other mechanistic arguments that are not needed and unsupported. In the process, the elementary theory is discounted without justification.

The example in Fig. 13 was chosen because the results <u>do</u> conform moderately well to elementary theory when fully interpreted. However, it was noted that the theory does not explain the weak pressure dependence that is manifested unless one allows that the response function is pressure dependent. The elementary response function theory prescribes a pressure dependence through a factor n, i.e., $\mathcal{R} = nf(\Omega)$. At pressures typical of L^* instability, n (the pressure exponent in the burning rate law) is usually mildly pressure dependent, so that a small spread of the data with pressure in Fig. 13 is to be expected. However, it is generally recognized that the elementary response function theory does not adequately describe the dependence of response on mean pressure, and the "pressure spread" in the $L^* (\bar{r})^2$ vs Ω plot can show this rather dramatically. This is illustrated in Fig. 14, which is based on the data of Ref. 4 for another propellant. In this figure, several points emerge from the examination of the original data:

a) There is a large spread of the data according to pressure, with high pressure data on the right.
b) When allowance is made for pressure dependence, the trend of the data for each pressure is similar to Fig. 13 (i.e., conforms to the elementary theory).
c) Examination of the original data for either Fig. 13 or 14 shows that there is a great deal of scatter in the trend of α along the $L^* (\bar{r})^2$ vs Ω curves. While high - α results tend to be at higher Ω and lower $L^* (\bar{r})^2$ in accord with the theory, one would be hard pressed to mark off an "α scale" along the curve.
d) In tests where repeated burns with growing oscillations occurred spontaneously (Fig. 15), the successive α's often <u>increased</u> between

burn #1 and burn #2, followed then by decreasing α (with increasing L^*) in subsequent burns as predicted by theory. Since the first burn seems to behave in an anomalous manner, and most tests have only one or two burns, the trends of all data that depend on α will be affected by this anomalous (but heretofore unmentioned) first burn effect.

From the foregoing, it is evident that any plot of any variables that depend on the response function will show a trend with pressure or mean burning rate that is contrary to the elementary theory if (as is usually the case) the response function is pressure dependent. An example of such a plot (from Ref. 4) is shown in Fig. 16. The authors of this reference looked on the trend of this data as anomalous because of the steep rise in trend of frequency with burning rate for propellants with bimodal AP particle size. It was speculated that this reflected a different form of the response function than given by the QSHOD theory, a speculation that triggered investigation of the idea that a bimodal size distribution might give a response function with double peaks. However, the trend of the data could equally well be explained by the widely accepted recognition that the response function can be pressure dependent, i.e., the anomalous steep trends in Fig. 16 are clearly a systematic trend with pressure. In fact, one of the propellants (A-146) for which "anomalous" results are claimed in this figure is the same propellant (same tests) leading to the correlation in Fig. 13, which shows rather good agreement with the elementary theory. Thus, one is led to the conclusion that the test results need to be examined more fully before drawing conclusions regarding the existence or plausible cause of divergence from elementary theory.

Curiously enough, the authors of Ref. 4 issued a later report concerning the same experimental data that has apparently escaped notice, in which it was noted that the steep upward trend in data in Fig. 16 was associated with a trend to high values of α. It was noted that at the higher burning rates (higher pressures), it was not possible to get oscillations at low α, except occasionally with negative α after an ignition peak. An explanation of this trend of oscillatory behavior was offered, based on the elementary theory. It was shown that, for suitable values of the parameters A and B in the QSHOD response function model, two different kinds of stability limits occur. Under conditions corresponding to the low burning rate tests in Fig. 16, α decreases as L^*

increases (at a given mean pressure and $\bar{r}$) until $\alpha = 0$ is reached. At higher burning rate, α decreases with increasing L^* until some value of L^* is reached beyond which the value of α jumps to negative values (no oscillations). The region of steep increase in α with $\bar{r}$ in Fig. 16 is thus in complete accord with elementary theory, and simply reflects the second kind of stability limit, that had escaped notice in earlier (and subsequent) studies. The manifestation of this second kind of stability limit is illustrated by the A = 16 curve in Fig. 17, reproduced from Ref. 5.

The studies described in Ref. 4 and 5 were closed out leaving interpretation incomplete, only partially published in the archival literature, and with results that have challenged later investigators. One such result is an oscillatory behavior typified by Fig.18 (from Ref. 5 and later published in Ref. 6). In this test a spontaneous transition from high to low frequency occurred during a test. In 1986 the present author (Price) returned to this result and the "second kind" of stability limit predicted by the elementary theory in Fig. 17. Computations of the variables of Fig. 17 vs Ω gave a clearer picture of the second kind of stability limit and what happens during a test as L^* increases during burning. Figure 19 shows the trends of (A'/κ) $(L^* r^2)$ vs Ω and $\kappa(\alpha/r^2)$ vs Ω for two combinations of the QSHOD parameters A and B and various values of pressure exponent n. The top example shows trends for "first kind" of stability limit, i.e., as L^* is increased, α decreases until a critical value of L^* and Ω is reached where $\alpha = 0$. The bottom graph shows Ω to be triple valued in Ω over a certain range of L^*, meaning that in this range of L^*, three different oscillation frequencies are possible. Since α is highest at the highest of these frequencies, it is the one likely to be manifested, provided the value of (A'/κ) $(L^* r^2)$ does not exceed the local maximum shown in the figure. However, in a test in which the increasing L^* (during the test) carries it past the maximum, oscillation must jump to the low Ω part of the L^* curve, with an abrupt transition to low frequency as in Fig.18. Thus the "anomalous" result of Fig. 18 is seen to be a further manifestation of the behavior responsible for the "second kind" of stability limit, differing only in that the frequency jump occurs under conditions where $\alpha > 0$ on the lower branch of the L^* curve (in the example shown in Fig. 19, a slightly higher value of n is necessary than the n = .5 example, for α to be > 1 on the low Ω branch of the L^* curve).

From the foregoing, it is evident that some of the "anomalous" results of the past are actually interpretable by the elementary theory, while more of the data is interpretable via elementary theory augmented by the widely recognized dependence of response function on pressure. Most reported results are too incomplete to constitute a test of theory. Some of the reported failings of the elementary theory have to do with the assumption that the combustion zone of the propellant is thin, an assumption that is used to decouple the treatment of combustion response function from the treatment of the combustor cavity oscillation. It is this assumption that makes it possible to model the combustor flow dynamics by a conservation of mass equation. However, the thin combustion zone assumption is clearly not applicable for some propellants such as double base, nitramine, or aluminized propellants. There are L^* instability models in the literature that do not use the thin combustion zone assumption, and add a conservation of energy equation in the model. These models have not been compared with experimental results, and the data from published works is not sufficient to provide a test of these models. As a result, our review did not include evaluation of these models.

We have discontinued our attempt to achieve a decisive "treatise" on this simplest of combustor instability problems, because we found that the results in the literature are insufficient for the purpose. We plan to write a technical note for a journal, highlighting the issues described here.

COMBUSTION OF AP-PBAN SANDWICHES WITH AP-FILLED PBAN LAMINAE

Extensive studies have been made in the past of edge burning of AP-binder "sandwiches," used as a model propellant system that is much easier to test and understand than a propellant made from particulate ingredients (e.g., Ref. 1, 7 8). These studies have contributed greatly to understanding of the combustion mechanisms of propellants. Some exploratory tests have now been made on the feasibility of studying the interaction of oxidizer/fuel flamelets in the propellant combustion zone. This interaction between adjacent large and small particles is believed to be an important determinant in ballistics of propellants, and a difficult aspect of the combustion to represent in propellant combustion models. The strategy here is to add particulate AP to the binder

lamina of sandwiches and see what effect it has on burning rate. In such tests, the oxidizer laminae play the role of large AP particles, and the filled binder lamina corresponds to the fine AP filled matrix between large particles in the propellant. It is relatively easy to test the effects of ratio of AP to binder in the lamina, the effect of particle size, and of thickness of the matrix lamina. Using the well developed understanding of combustion of conventional sandwiches as a starting point, it should be possible with the new test results to clarify the three-dimensional flame interaction in propellants.

An initial series of tests was conducted at 500 psi on sandwiches with a 1:1 ratio of 10 μm AP and PBAN binder in the binder lamina. Fig. 18 shows the dependence of burning rate on binder lamina thickness. Also shown is the burning rate for sandwiches with pure PBAN binder laminae (from Ref. 8). Notable is the fact that in the range of binder thickness usually tested with pure binder laminae, the burning rate with the AP-filled binder is lower, and that the curve for filled binder has a maximum at a lamina thickness more than three times that for pure binder. The AP-PBAN matrix is too fuel rich to burn on its own, so these effects necessarily depend on interaction with the AP lamina flame. Further, the 10 μm particles are too small to have individual flamelets, and the particle and binder vapors are believed to be fairly homogenously mixed by the time they reach the leading edge O/F flame normally present in the region above the contact surface of the AP and binder lamina (Ref. 8). The principal interaction effects are:

a) Heat loss from the AP to the binder lamina (normally present with pure binder laminae). The AP-filled lamina has a higher heat capacity and thermal conductivity than pure binder, which would tend to reduce burning rate when it is vaporizing endothermally.

b) The oxidizer vapor in the fuel flow tends to shift the stoichiometric surface in the oxidizer-fuel vapor mixing region toward the fuel flow, causing the leading edge of the O/F flame to be correspondingly shifted. For thin laminae, this effect is small, but with thick laminae the flame shifts to a location above the lamina contact plane, most favorable for high rate (Fig. 20).

c) At large binder lamina thickness, the central part of the lamina acts as a heat sink, with efflux liberating heat too far from the surface to affect burning rate. Lateral heat drain (in the solid) from the rate controlling region reduces burning rate.

The foregoing three arguments appear to explain the trend of burning rate with lamina thickness in Fig. 19. They will have to be elaborated to accommodate future results (at different pressures, with higher O/F ratio, and larger AP particle size). Tests are now in progress on sandwiches with particles in the binder lamina that are large enough to have their own attached O/F flamelets.

REFERENCES

1. Price, E. W., Handley, J. C., Panyam, R. R., Sigman, R. K., and Ghosh, A., "Combustion of Ammonium Perchlorate-Polymer Sandwiches," AIAA Journal, vol. 19, March 1981, pp. 380-386.

2. Deur, J. M., and Price, E. W., "A Surface-Coupled Flamelet Approach to Dynamic Response in Heterogeneous Propellant Combustion," AIAA Paper 88-2938, July 1988.

3. Price, E. W., "Experimental Observations of Combustion Instability," Fundamentals of Solid-Propellant Combustion, Vol. 90 of AIAA Progress Series, AIAA, August 1984, pp. 733-790.

4. Beckstead, M. W., Boggs, T. L., Crump, J. E., Dehority, G. L., Hightower, J. D., Kraeutle, K. J., Krier, H., Mathes, H. B., and Price, E. W., "Combustion of Solid Propellants and Low Frequency Combustion Instability, Progress Report 1 April - 30 September 1967, Naval Weapons Center TP 4478, April 1968.

5. Boggs, T. L., Price, E. W., Mathes, H. B., Kraeutle, K. J., Dehority, G. L., Crump, J. E., and Culick, F. E. C., "Combustion of Solid Propellants and Low Frequency Combustion Instability, Progress Report 31 October 1967 - 1 November 1968" Naval Weapons Center TP 4749, June 1969.

6. Boggs, T. L., and Beckstead, M. W., "Factors of Existing Theories to Correlate Experimental Nonacoustic Combustion Instability Data," AIAA Journal, Vol. 8, April 1970, pp. 626-631.

7. Hightower, J. D., and Price, E. W., "Experimental Studies Relating to the Combustion Mechanism of Composite Propellants," Astronautica Acta, Vol. 14, Nov. 1968, p. 11.

8. Price, E. W., Sambamurthi, J. K., Sigman, R. K., and Panyam, R. R., "Combustion of Ammonium Perchlorate-Polymer Sandwiches," Combustion and Flame, Vol. 63, 1986, pp. 381-413.

Table 1
Measured Values of Smooth Band Width

Binder Thickness	200 psi	400 psi	500 psi	600 psi	700 psi
154.000	257.000	Single crystal AP, Markou			
147.000	235.000				
140.000	220.000				
125.000	206.000				
118.000	191.000				
110.000	184.000				
200.000	276.000				
155.000	231.000				
180.000	267.000				
35.000	70.000	Pressed AP, Markou			
60.000	110.000				
50.000	80.000				
44.000	62.000				
39.000	55.000				
55.000	65.000				
51.000	60.000				
21.000	35.000				
28.000	56.000				
20.000	42.000	Pressed, Panyam			
33.000	57.000				
90.000		120.000	Pressed, Markou		
80.000		110.000			
60.000		90.000			
155.000		222.000	Pressed,		
167.000		200.000			
140.000		180.000	Panyam		
120.000		170.000			
52.000			81.000	Single crystal, Markou	
68.000			118.000		
59.000			92.000		
48.000			68.000		
45.000			61.000		
39.000			56.000		
108.000			169.000	Pressed, Markou	
100.000			154.000		
85.000			138.000		
54.000			92.000		
65.000			111.000		
62.000			Pressed, Markou	92.000	
77.000				115.000	
79.000				Pressed, Markou	111.000
93.000					126.000

Table 1 - Continued

Binder Thickness	900 psi	1000 psi	1200 psi	75 psi	150 psi	100 psi	300 psi
111.000 85.000	111.000 100.000	} Pressed, Markou					
69.000 62.000		85.000 81.000	} Single crystal, Markou				
76.000 91.000			80.000 100.000	} single crystal Markou			
38.000			46.000	} Pressed, Markou			
21.000 19.000				37.000 35.000			
24.000 21.000			Pressed		45.000 41.000		
18.000			AP,			52.000	
33.000			Pany am				52.000
98.000							115.000
62.000 92.000							100.000 123.000

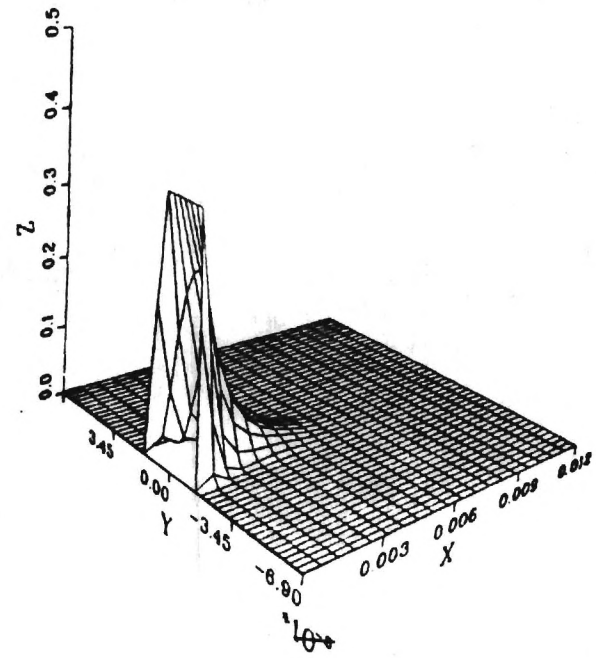

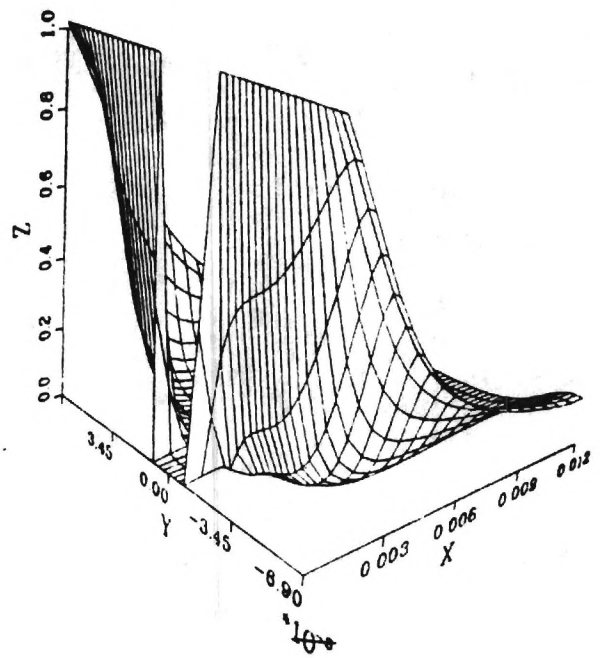

Fig. 1 Concentration field for methane (gets broken down to CH_3). (top figure)

Fig. 2 Concentration field for oxygen. (bottom figure)

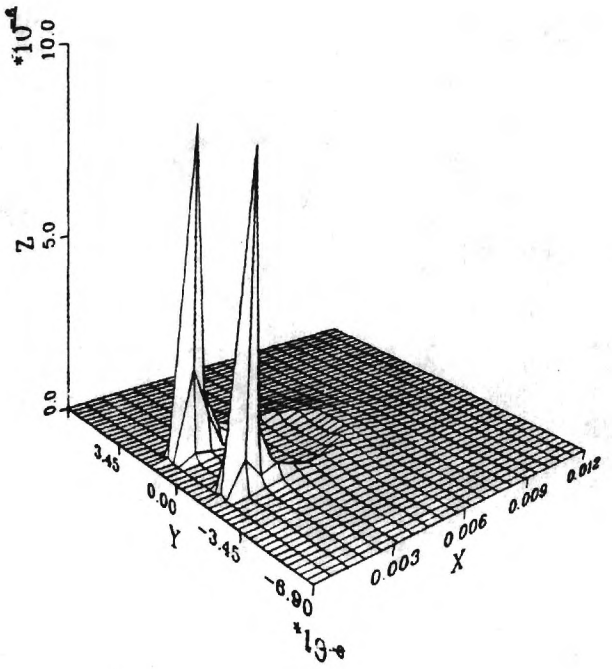

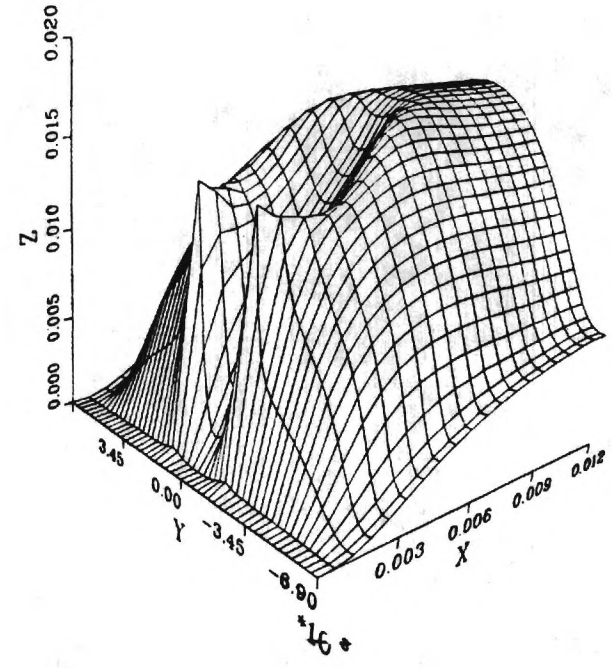

Fig. 3 Concentration field for short-lived intermediate product (CHO: peaks are due to extremely high volumetric reaction rate in LEF).
(top figure)

Fig. 4 Concentration of H_2O.
(bottom figure)

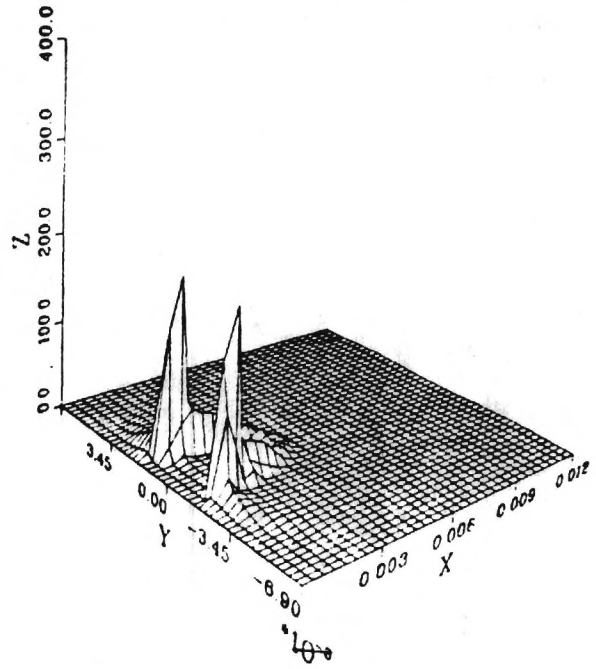

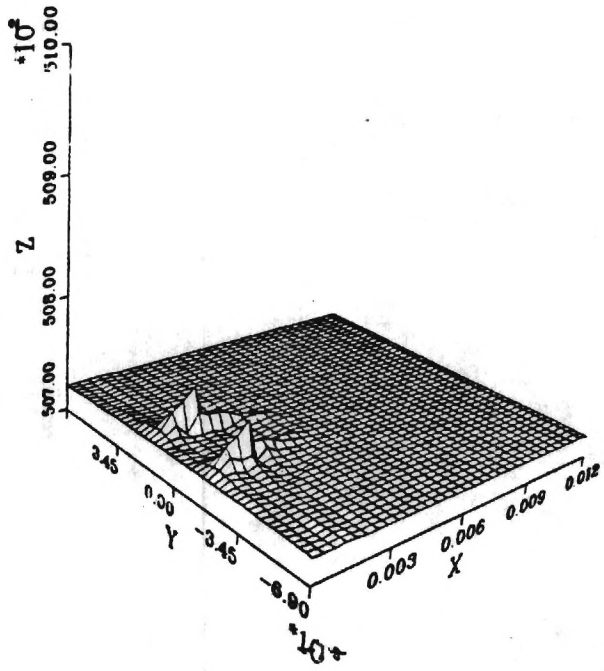

Fig. 5 Heat release rate per unit volume.
(top figure)

Fig. 6 Pressure (peaks are in LEF, due to high volumetric expansion; leads to diverging flow approaching LEF).
(bottom figure)

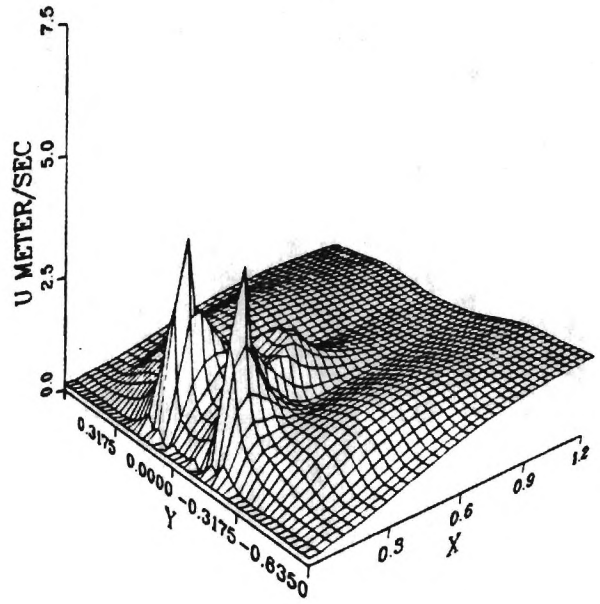

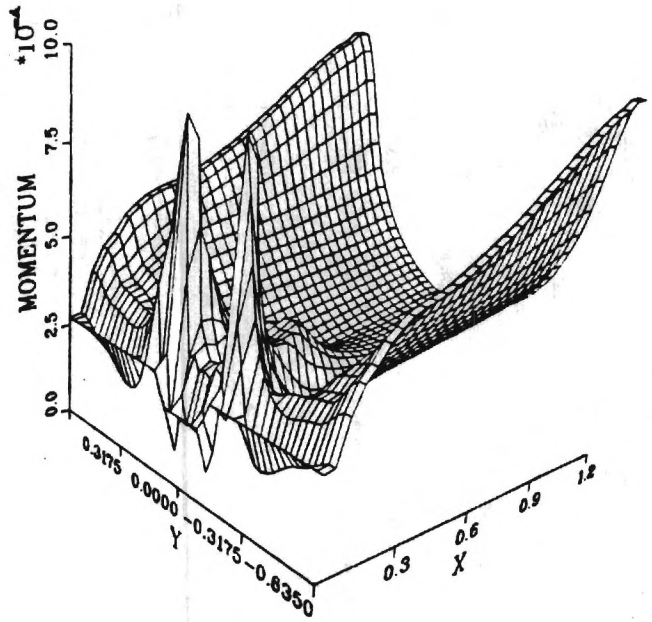

Fig. 7 Axial component of velocity.
(top figure)

Fig. 8 Axial component of momentum (decreases where the flow is into a rising pressure).
(bottom figure)

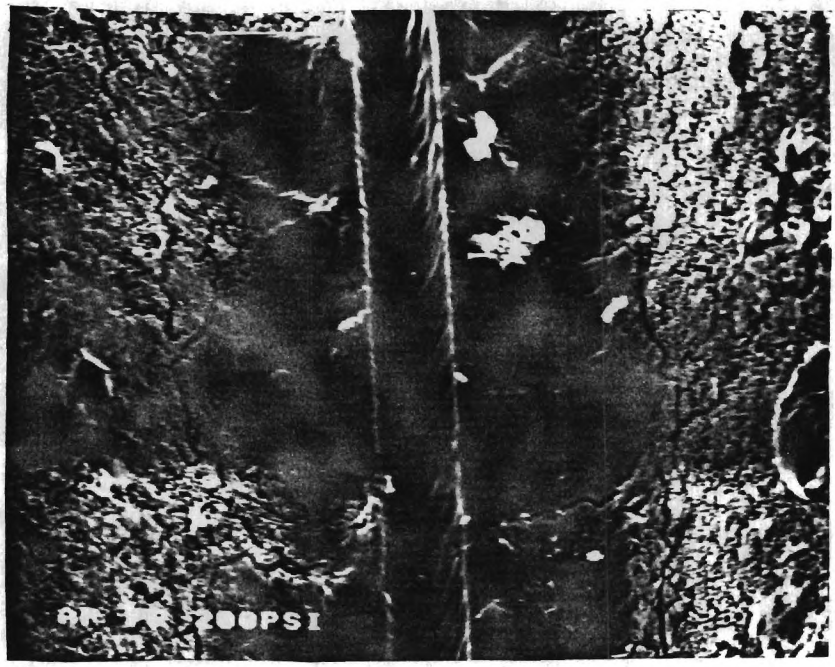

(a)

(b)

Fig. 9 Quenched samples showing the "smooth band."
a) Quenched sandwich.
b) Quenched propellant.

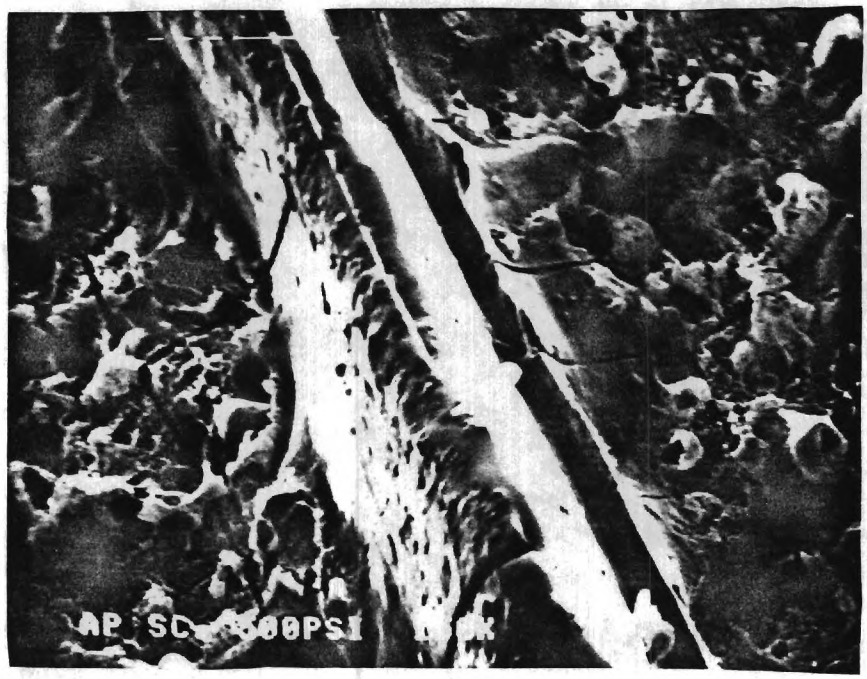

(a)

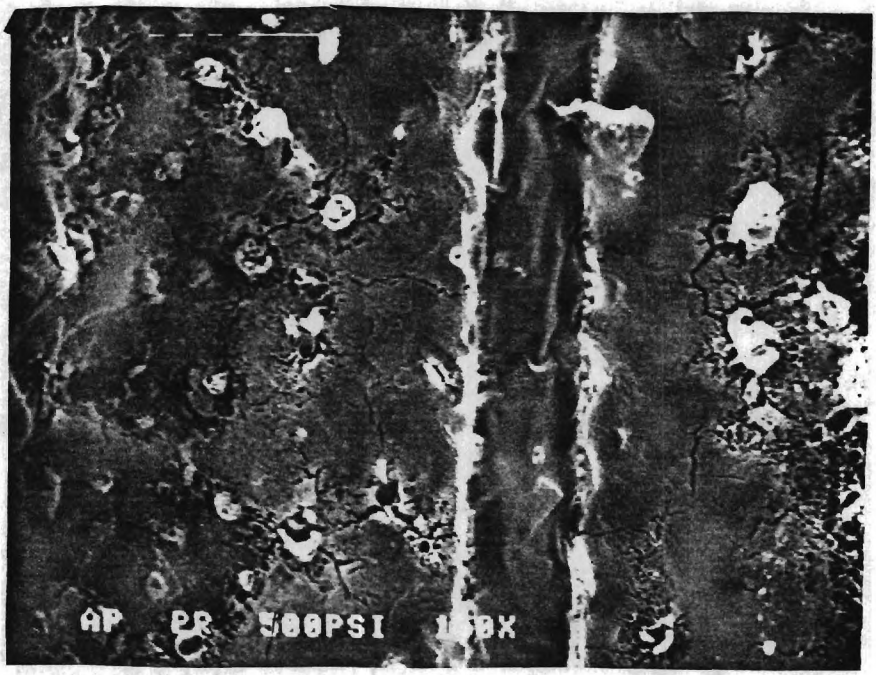

(b)

Fig. 10 Quenched sandwich surfaces.
a) Single crystal AP laminae (example of AP-binder delamination during quench).
b) Pressed AP laminae.

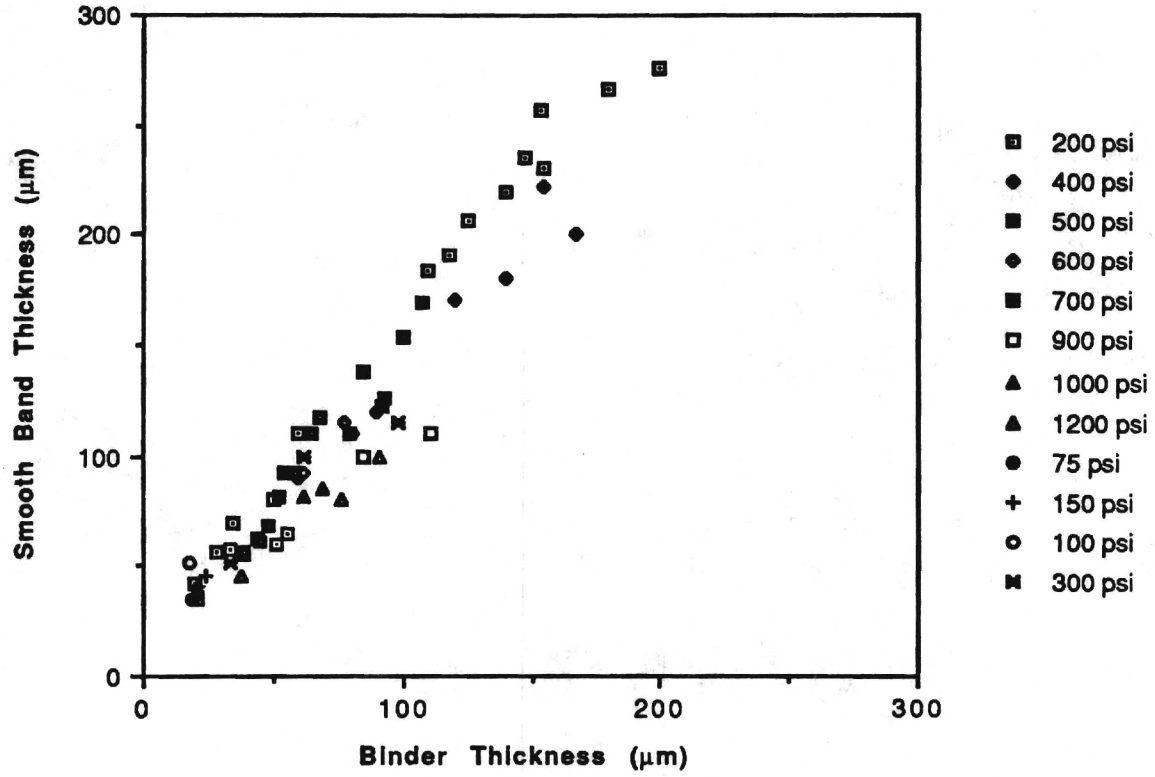

Fig. 11 Experimental results showing smooth band width vs binder lamina thickness.

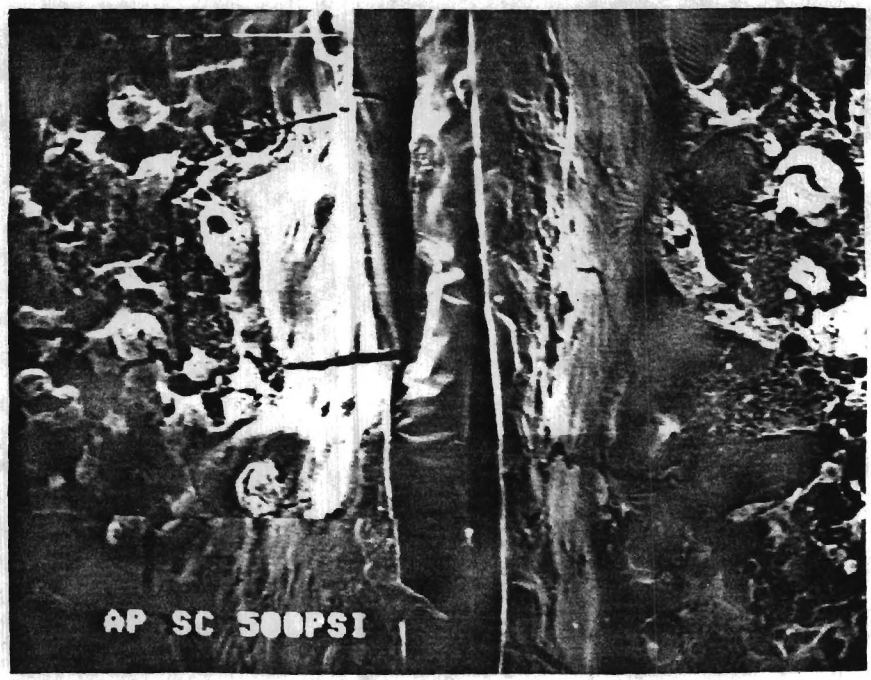

Fig. 12 Quenched sample with lamina separation switching from one AP lamina to the other.

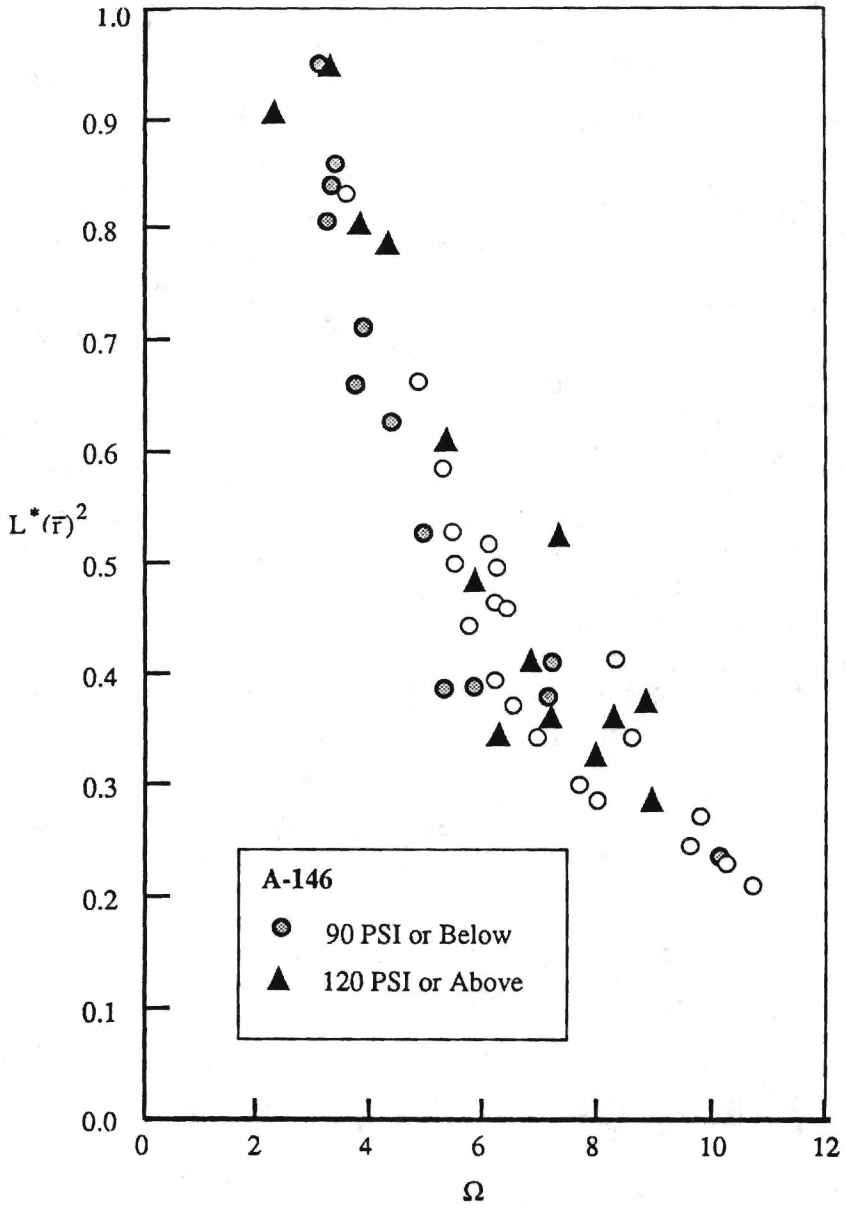

Fig. 13 Correlation of $L^* (\bar{r})^2$ and Ω for A-146 propellant in L^* instability tests (data from Ref. 4).

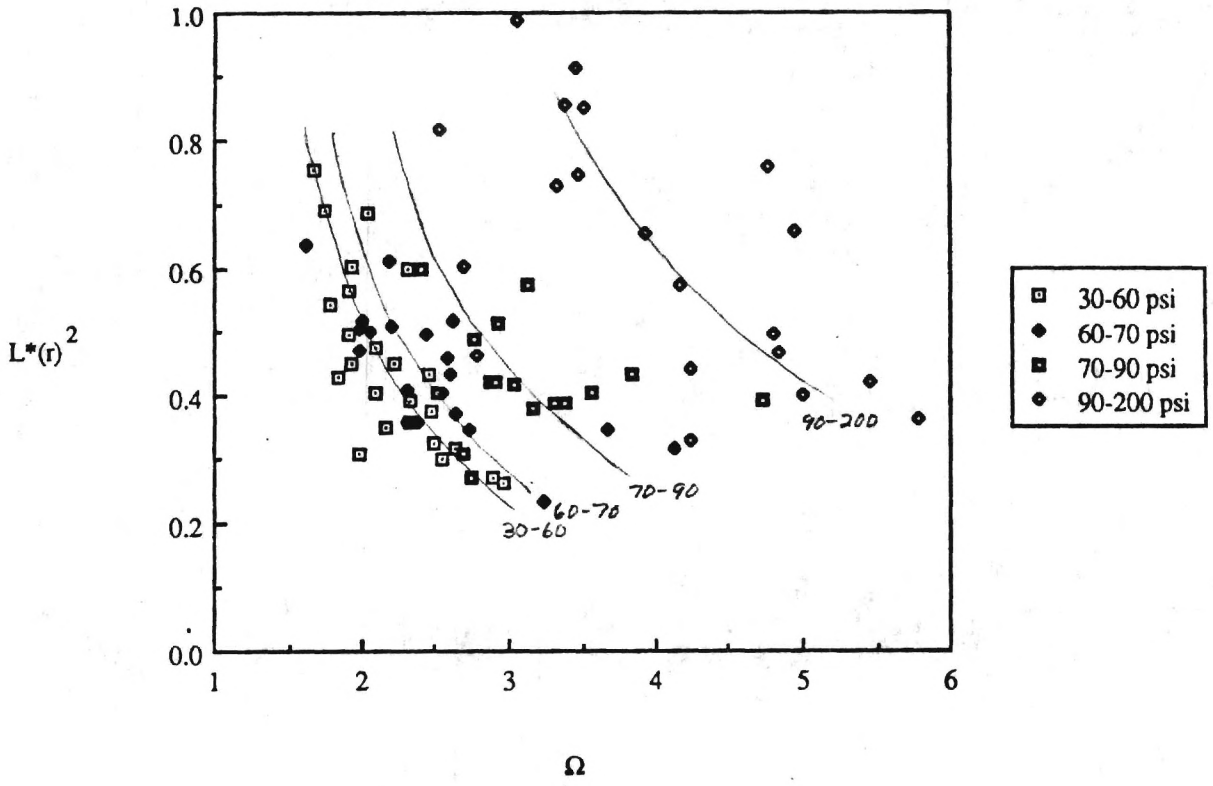

Fig. 14 Correlation of L^* $(\bar{r})^2$ and Ω for A-167 propellant in L^* instability tests (data from Ref. 4).

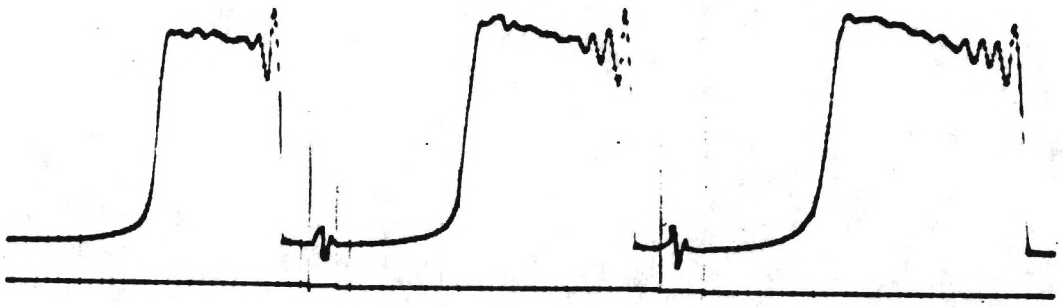

Fig. 15 Pressure-time curve for an L^* instability test in which oscillations repeatedly caused quench, followed by spontaneous reignition.

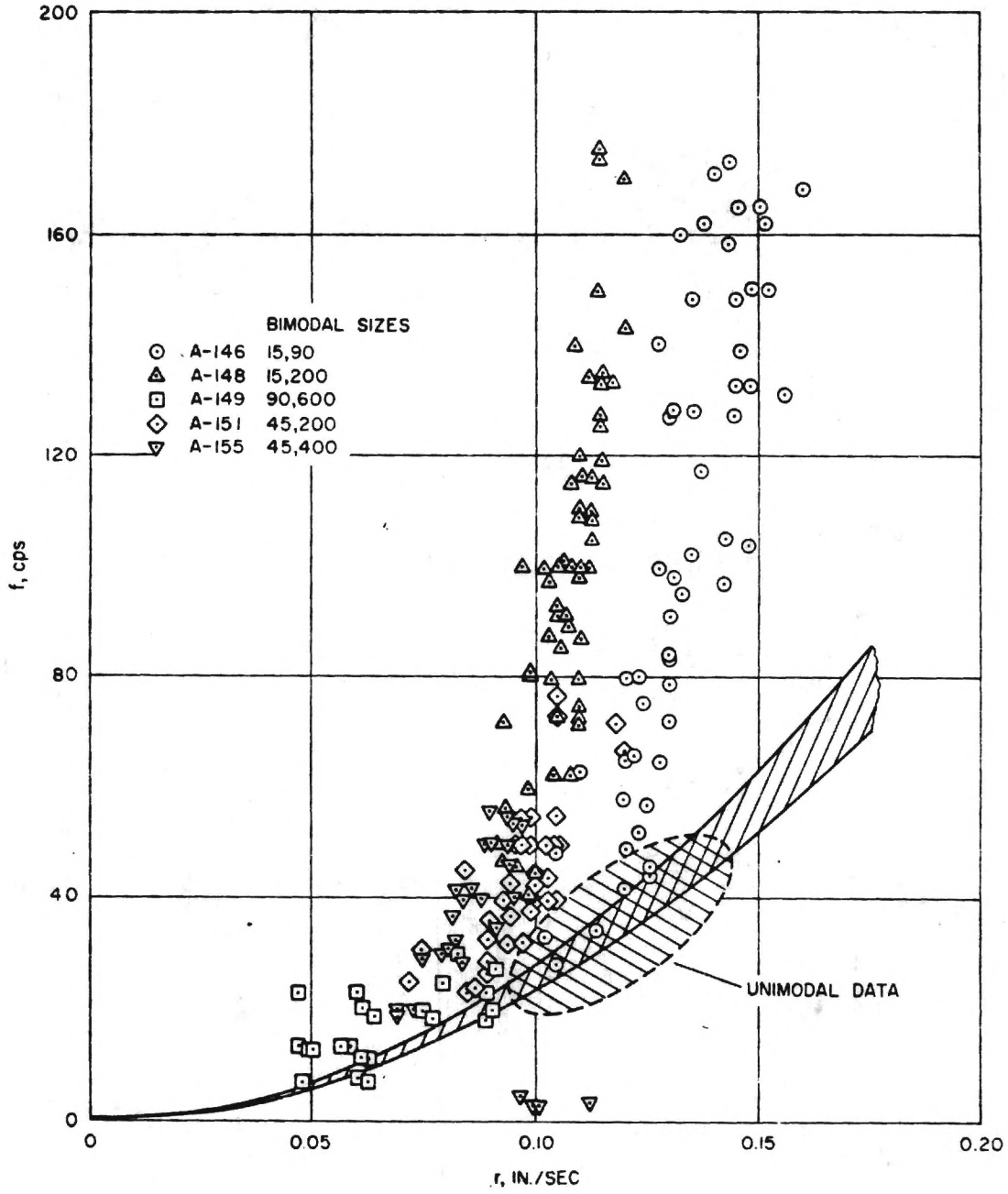

Fig. 16 Correlation of frequency and mean burning rate during L^* instability for several propellants (from Ref. 4).

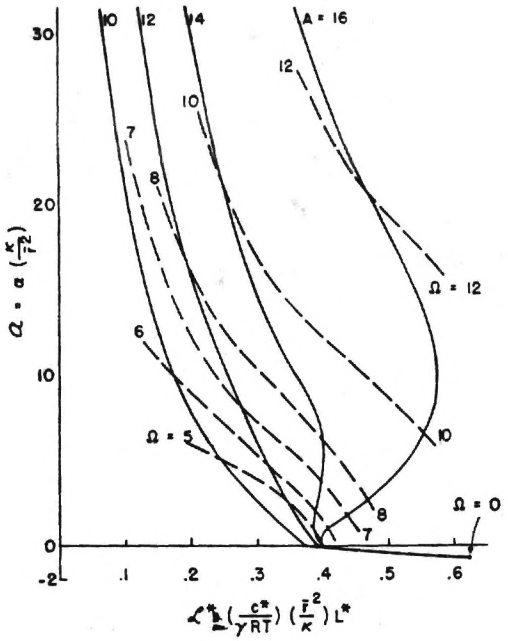

Fig. 17 Figure from Ref. 5 showing nondimensional α versus nondimensional L^* for B = .8 and various values of A in the QSHOD response function model. Curves for A = 14 and A = 16 show the "second kind" of stability limit.

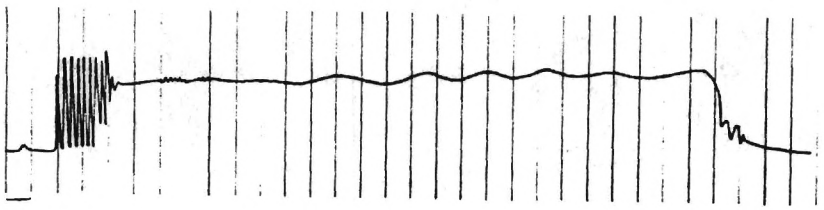

Fig. 18 Pressure-time curve for instability experiment in which a spontaneous abrupt change in oscillation frequency occurred (from Ref. 5).

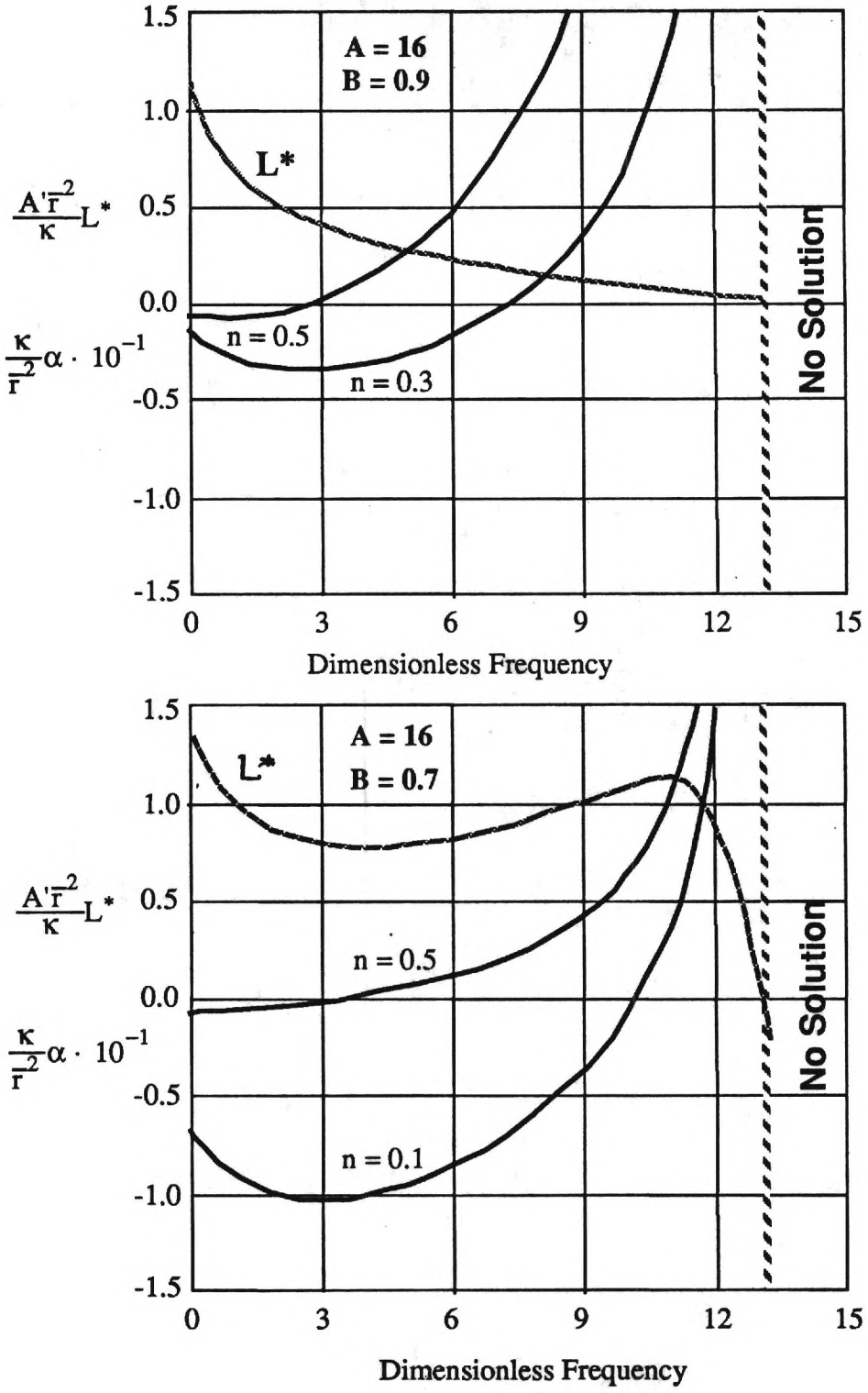

Fig. 19 Plots of L^* and α vs Ω that show a region of L^* for which there are solutions for multiple values of Ω (curve based on QSHOD theory). Note that as L^* increases during a test (on the right), a jump to lower Ω is necessary if L^* reaches the value at the maximum on the right.

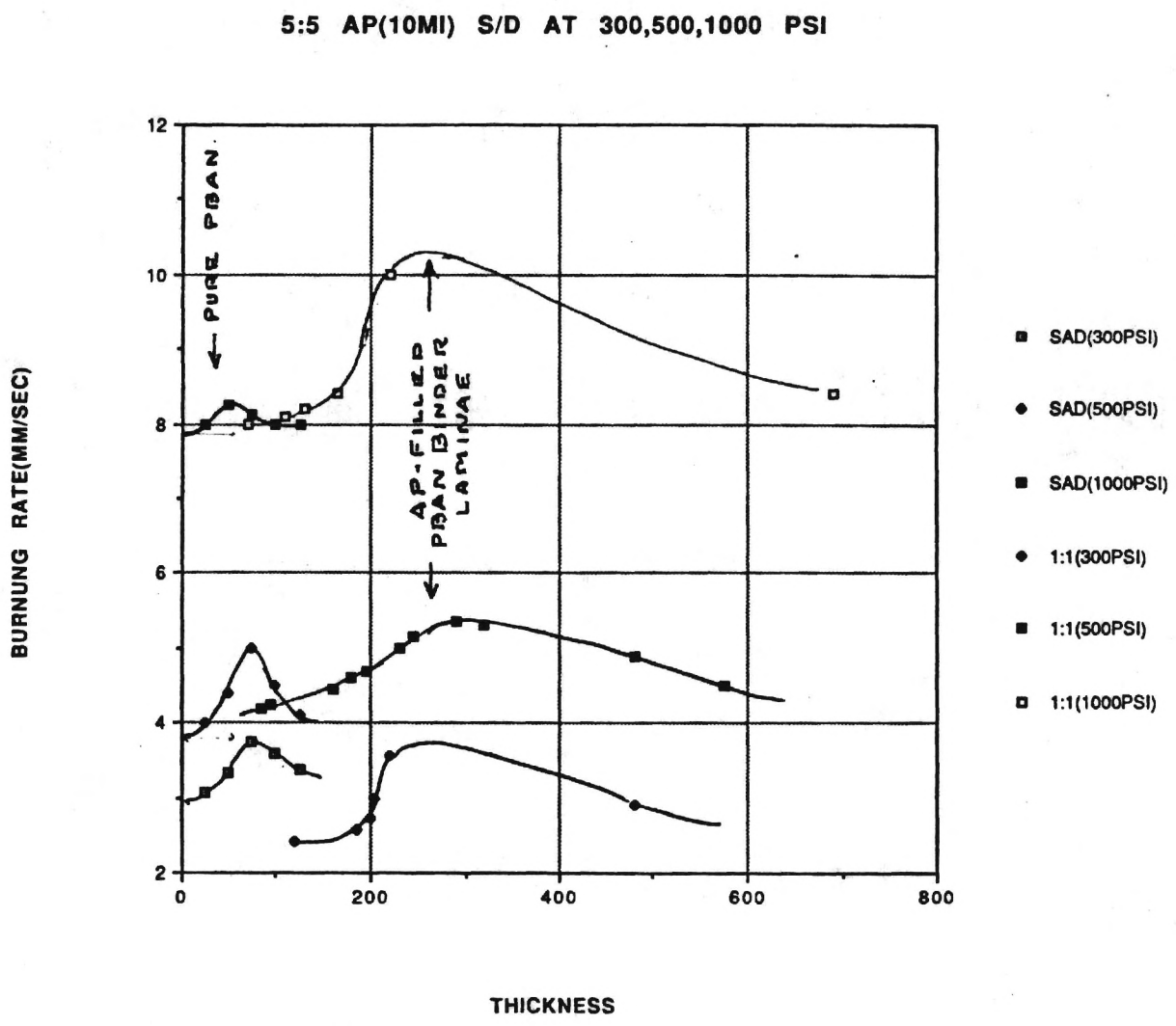

Fig. 20 Burning rate of AP-PBAN polymer sandwiches (Ref. 7) and similar sandwiches in which the binder laminae consisted of a 50-50 mix of PBAN and 10 μm AP.

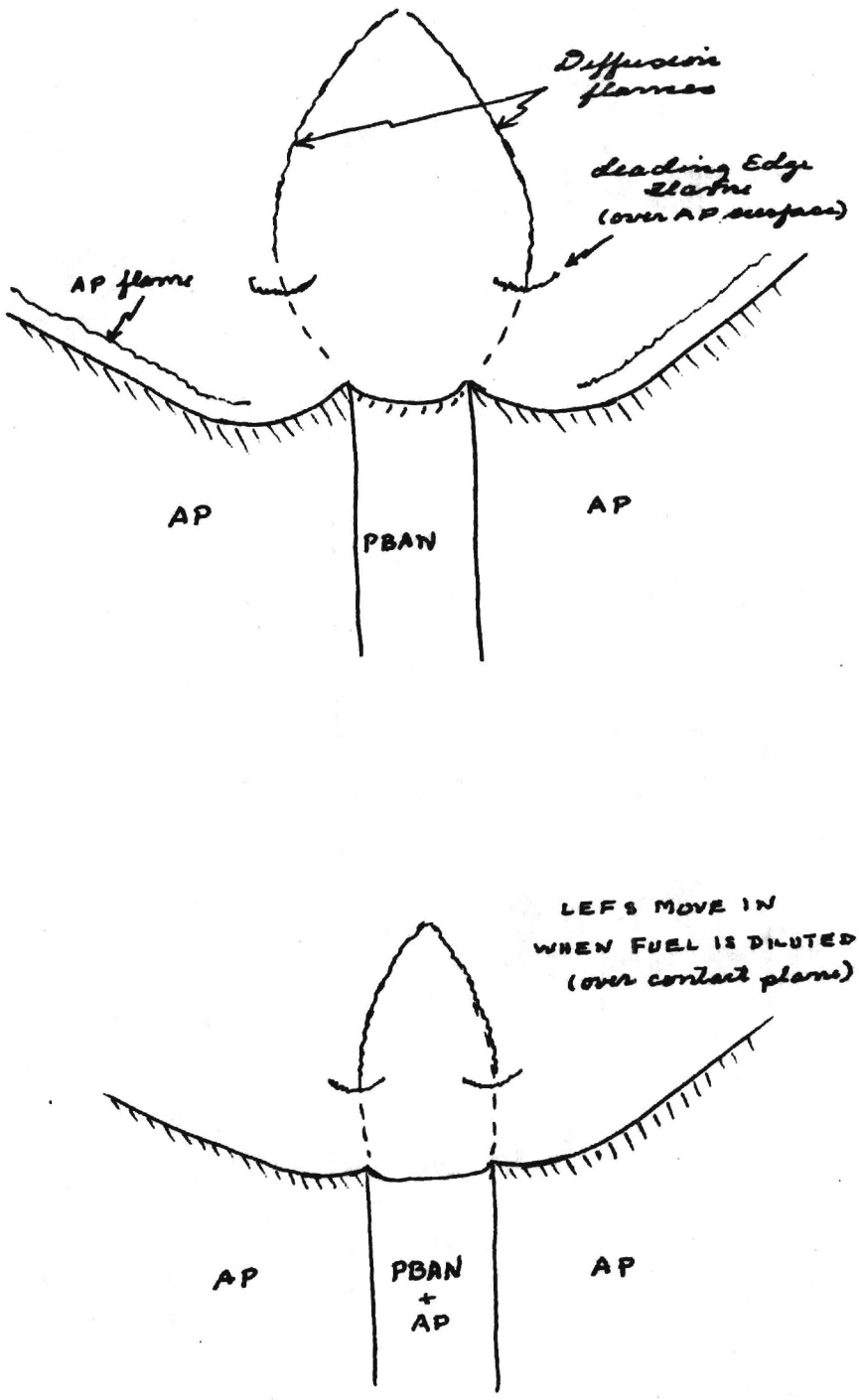

Fig. 21 Sketch of the flame complex for AP-PBAN sandwiches, comparing the complex for pure binder laminae and AP-filled binder laminae.